COMSOL CONFERENCE 2024 BOSTON

Thermal Modelling of Large Thin Film PZT MEMS Micro Actuator Arrays

Mani Sivaramakrishnan
ARNDIT LLC, Portland, OR 97229, USA.

Abstract

Thermal modelling of an industrial thin film piezo-MEMS inkjet die containing a large array of micro-actuators is presented. The paper highlights the challenges involved in modeling of a large size die (32 mm x13mm x0.5 mm) keeping the details of the very small actuators (55 µm x 1 mm x 5 µm). The predicted die temperatures are compared with the experiment. On the other hand, modelling provides further insight into some aspects (e.g. the local temperature distribution of the actuators) which are difficult to measure.

Keywords: piezo-MEMS, inkjet, actuators, thermal modelling, PZT.

Introduction

Large arrays, typically consisting of thousands of devices, made from thin film PZT MEMS technology are increasingly being used in several applications including industrial inkjet printers, adaptive optics and so on. Thin film PZT is attractive because of lower operating voltages and smaller form factors. Despite the smaller operating voltage, thin film devices are operated at much higher electric fields (larger than the coercive field) and at higher frequencies. Hence, there is significant self-heating that occurs in thin film arrays. In these arrays, heat is generated in very small volumes of the individual micro actuators, but heat dissipation takes place at the scale of the overall dimensions of the die. This presents a challenging problem in the thermal modelling of such arrays since both the small size of the micro actuator and the large dimensions of the overall die must be accurately represented in the model. In this paper, we report the results of thermal modelling of an industrial inkjet printhead die (32 mm x13mm x0.5 mm) consisting of 1420 Thin Film PZT-based micro actuators (55 µm x 1 mm x 5 µm).

Experimental Set Up / Measurements

An industrial inkjet thin film piezo-MEMS die consisting of a large array of 1420 micro-actuators was used as a test die in this study. The array itself is arranged in four rows with 355 actuators in each row. The overall size of the die was 32 mm x13 mm x 0.5 mm. Most of the measurements were performed on a single row of actuators. Electrical contacts were made to every sixth (1st, 7th, 13th etc.) actuator and the whole row was electrically divided into three groups, with each group containing twenty actuators. All the actuators in each group were electrically connected. Each test group (left, center, or right) could be driven alone or in combination with the others. A schematic view of the die representing the different groups of actuators is shown in Fig. 1. The die also includes two temperature sensing elements at the ends of each row for *in-situ* temperature measurements. To make sure that the measured temperature corresponds to well-defined thermal boundary conditions, the die was firmly attached to a polycarbonate substrate. This is very important for a comparison between the measured and the modelled temperatures.

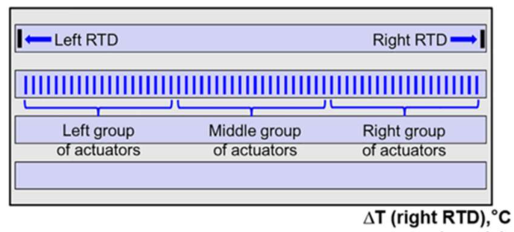

Figure 1. Schematic top view of the die illustrating different groups of actuators

Seven different firing schemes ('a' through 'g') involving different combinations of groups of actuators were used in this experiment, as illustrated schematically in Fig. 2. The groups of actuators that are fired are shown in red and the unactuated groups in blue. A sinusoidal waveform with an amplitude of 25 V and DC offset of 25 V at a frequency of 100 kHz was used to drive the actuators. The steady state temperature rise for each combination of firing as measured by one of the temperature sensors on the die is also shown in Fig. 2.

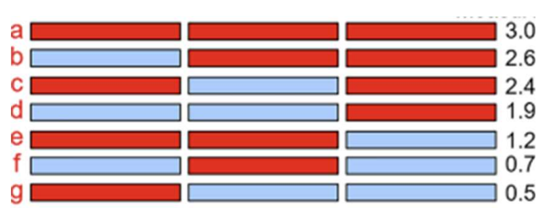

Figure 2. Different actuation schemes (a through g). Each bar represents a group of actuators. The red bar represents an actuated group, and the blue bar, an idle group. The numbers on the right are the temperature rise as measured by the in-situ temperature sensors.

COMSOL Thermal Model and Simulation

A 3D finite element model of the die together with the substrate holder was developed in COMSOL ver. 6.2. As mentioned earlier, this is a fairly complex die consisting of a large array of actuators. Each actuator is made up of several proprietary layers including the main thin film PZT layer where the heat is generated during actuation. We start building the model with a single actuator with accurate dimensions and then use the array forming techniques in COMSOL geometry tools to build the entire row with a high fidelity. This not only simplifies the construction of the overall geometry with full details of the micro-actuators, but also makes the meshing easier. To keep the overall mesh size within manageable limits, only the actuated row is represented with full details of the individual actuators while treating the other rows simply as silicon. The full meshed geometry in COMSOL is shown in Fig. 3. A zoom-in view of a few actuators in the modelled geometry is shown in Fig. 4.

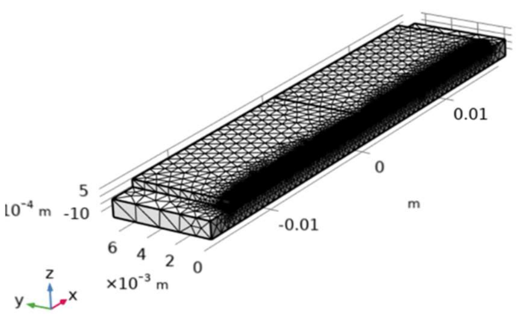

Figure .3 Overall meshed geometry of the MEMS die mounted on a polycarbonate substrate for thermal modelling.

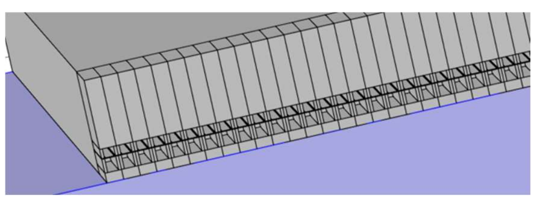

Figure 4. Zoom-in view of a few micro actuators in the modelled geometry.

P-E hysteresis measurements were also done at an individual actuator level using the same sinusoidal waveform used in the thermal measurements. The area inside the loop corresponds to the energy dissipated by a single actuator per cycle and this was used as the heat generation rate inside the volume of the actuator in the thermal model.
Two different heat dissipation mechanisms were considered in the model: the convection from all the ambient-exposed surfaces of the die and the conduction through the die and the polycarbonate substrate. The ambient as well as the bottom surface of the substrate were assumed to be held at 20°C. The radiation loss was neglected since the measured temperature rise of the die in this study was small (~ 10º C).

Simulation Results / Discussion

The temperature distribution from the model along a line passing through the centers of a row of actuators in a direction parallel to the length of the die is shown in Figs. 5-7 for three different actuation schemes.

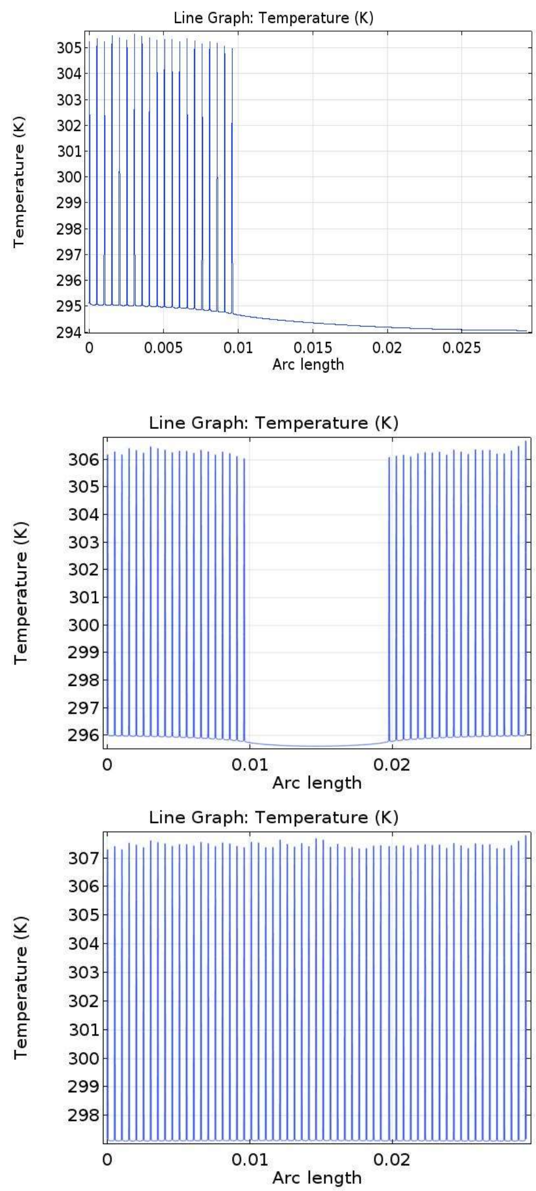

Figure 5. Temperature distribution from the thermal model along a row of actuators for three different actuation schemes: Top: Only the left group is fired (scheme 'g'); Middle: Both the left and the right groups are actuated (scheme 'c'); Bottom: All three groups are actuated (scheme 'a').

When the left group is alone actuated (scheme 'g'), the temperature at the left end of the die is slightly higher than that at the right end of the die, as expected. When both the left and right groups are actuated (scheme ‘c’), the temperature distribution is symmetrical with equal temperatures at both ends of the die, but higher than in the middle region of the die. When all the three groups (sixty actuators) are fired, once again the temperatures at both ends of the die are equal but higher than for all the other cases. A comparison of the temperature rise for all the seven schemes from modelling and measurement is shown in Table I.

Table 1. *Temperature rise from measurement and modelling for different actuation schemes*

Scheme	Temperature rise (ºC)	
	Measurement	Modelling
a	3	3.9
b	2.6	3
c	2.4	2.8
d	1.9	1.9
e	1.2	2.0
f	0.7	1.1
g	0.5	0.9

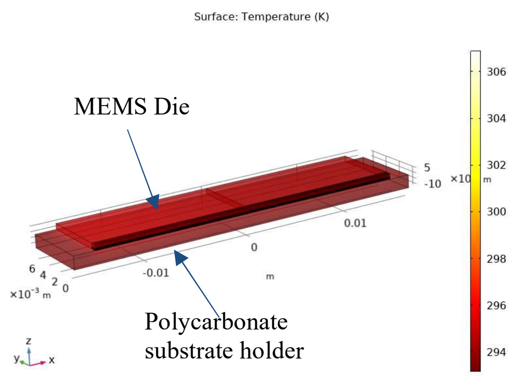

Figure 5. Temperature distribution of the full die and the polycarbonate substrate holder.

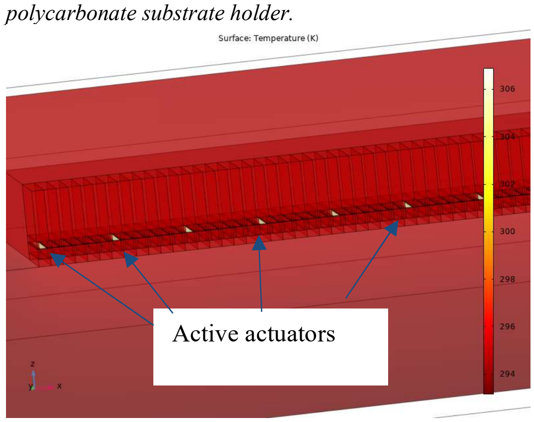

Figure 6. Zoom-in view of the temperature plot showing the hotter regions where the active actuators are located.

The modelling also shows that the local temperature at each fired actuator is about 10º C higher than the average temperatures at the ends of the die. This local temperature distribution is difficult to measure, and this is where the modelling is helpful in getting some insight. 3D surface plot of temperature of the full die and the polycarbonate substrate holder is shown in Fig. 5. The front of the die (closer to the viewer) is the row of active actuators. The red region at the back contains other rows of inactive actuators, but they are treated as Si for the sake of simplicity of modeling. A zoom-view of the same 3D-Temperature plot in Fig. 6 shows clearly the hotter regions where the active micro-actuators are located.

2D surface plot of temperature along a cross-section plane containing a few actuators is shown in Fig. 7. The local temperature at the micro actuator is clearly distinguished from the overall background of Si blocks (shown in blue).

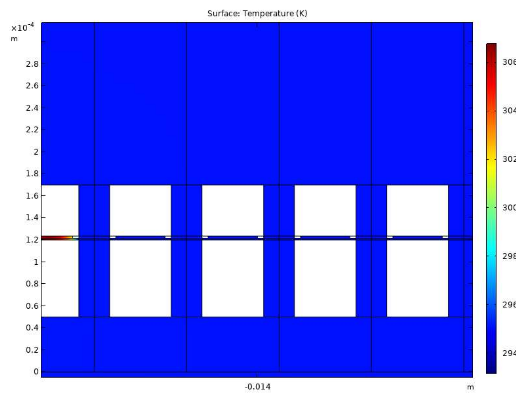

Figure 7. Temperature distribution along a cross-sectional plane containing a few actuators. Blue areas are Si. The actuated device appears red in color due to the hotter temperature.

Our modelling also shows that most of the heat dissipation (about 85 percent) takes place by conduction through Si and eventually through the polycarbonate substrate. Convection accounts for only the remaining 15 percent of the heat dissipation. This is the reason why the measured and modelled rise in temperatures of the die (see Table 1) are rather small. This underscores the importance of mounting the dies on good thermal sinks. If the die were kept floating in air, heat removal solely by convection (and possibly by radiation) would lead to a substantially higher temperature of the die, potentially destroying the device during operation.

Conclusions

Thermal modelling of an industrial piezo-MEMS inkjet die consisting of a large array of micro-actuators is presented. The main challenge in this modelling is the large size of the die as compared to the very small size of the actuators. Both the details of the micro-actuators and the overall size of the die must be faithfully represented in the model since the former governs the heat generation and the latter determines the heat dissipation. The modelled and the measured temperatures of the die are in good agreement. On the other hand, modelling provides insight into the local temperature distribution at the micro-actuators level which is difficult to measure.

References

[1] C. Fragkiadakis et al., "Heat Generation in PZT MEMS Arrays", Appl. Phys. Lett., 121, 162906 (2022).

Acknowledgements

The author wishes to acknowledge Dr. Peter Mardilovich and Dr. Carlos Fragkiadakis for sharing their measurement results included in this paper.